

Screening of high- Z grains and related phenomena in colloidal plasmas

O.Bystrenko, T.Bystrenko, A.Zagorodny

Bogolyubov Institute for Theoretical Physics, 03143 Kiev, Ukraine

Received April 3, 2003

Recent important results are briefly presented concerning the screening of high- Z impurities in colloidal plasmas. The review focuses on the phenomenon of nonlinear screening and its effects on the structure of colloidal plasmas, the role of trapped ions in grain screening, and the effects of strong collisions in the plasma background. It is shown that the above effects may strongly modify the properties of the grain screening giving rise to considerable deviations from the conventional Debye-Hückel theory as dependent on the physical processes in the plasma background.

Key words: *high- Z impurity, charged colloidal suspension, dusty plasma, nonlinear screening, bound ionic states, strong collisions*

PACS: *52.25.Vy, 52.27.Lw, 52.65.-y*

1. Introduction

Screening of charged objects embedded in a plasma background is one of the important problems of plasma physics, which attracted the attention of researchers during decades. Our interest in this issue is connected, first of all, with its implications in spatial ordering phenomena in colloidal plasmas (CP) such as dusty plasmas (DP) or charged colloidal suspensions (CCS). CP consist of a large number of highly charged ($Z \simeq 10^3-10^5$) colloidal particles of submicron size immersed in a plasma background. Experiments have revealed a number of collective effects in CP, in particular, the formation of Coulomb liquids or crystals associated with the strong Coulomb coupling in the colloidal subsystem [1–5]. It is clear that the properties of grain screening play therewith an important role, since the effective screened potentials produce the most significant contributions to the grain-grain interactions and thus determine collective properties of the colloidal component in CP.

The simplest approach conventionally employed in describing the grain screening in CP is the Debye-Hückel (DH) approximation, or, its modification for the case of the grain of finite size, the DLVO theory [6,7]. The DH approximation represents the version of Poisson-Boltzmann (PB) approach linearized with respect to the effective

potential based on the assumption that the system is in the state of thermodynamic equilibrium. The DH theory yields the effective interparticle interaction in the form of the so-called Yukawa potential which constitutes the basis for the Yukawa model.

Extensive molecular dynamics and Monte Carlo (MC) computer simulations performed for the Yukawa system (YS) [8–10] indicate that the latter makes it possible to explain the formation of condensed state in CP. However, it is clear that an accurate description of grain screening in CP requires more accurate approaches. Let us point out some important issues which should be primarily taken into account.

Firstly, these are the nonlinear effects in grain screening. Simple estimates evidence that the magnitude of the ratio $e\phi/k_{\text{B}}T$ (where e is the electron charge, ϕ is the potential, k_{B} and T are the Boltzmann constant and the temperature, respectively), which determines the significance of nonlinear effects, is of the order of $\simeq 10$ near the grain surface in real experiments on DP and CCS. This means that the linear approximation may fail in this case.

Secondly, a distinguishing feature of DP is that the charge of dust grains is maintained by plasma currents to the grain surface. Thus, DP are far from thermodynamic equilibrium even in the steady state. In these conditions, the Boltzmann distribution for plasma particles does not hold, which makes the equilibrium PB as well as the DH theory inapplicable. In other words, the kinetic description of grain screening is needed. Note that in this case the properties of grain screening may essentially depend on the presence of collisions in the plasma background.

It should be pointed out that the above issues have been the subject of numerous studies, where a number of important results have been obtained. The effects of nonlinear screening in the thermodynamically equilibrium case of CCS were studied in references [11–13]. It was found that in the presence of nonlinear effects, the effective potential at distances can be described by the linear Debye theory. However, the effective charge is smaller here than the bare grain charge.

A basic reference model for the case of collisionless plasma background with regard to the absorption of plasma particles by the grain, the OML theory, has been initiated by the paper of Bernstein and Rabinovitz [14]. As mentioned in this work, the asymptotic behavior of the screened potential for collisionless case is inversely proportional to the square distance. The authors also formulate here the question about the role of the bound ionic states in the grain screening. Later on the OML theory and the closely related collisionless approaches have been developed in numerous works [15–22]. The particular interest to the collisionless case is due to its industrial implications and due to the fact that the laboratory and astrophysical DP may be considered collisionless in most of the cases with a good accuracy. It was found that within the range of plasma parameters and grain sizes typical of the experimental observations, the effective potentials in the vicinity of the grain approach the predictions of DH theory, i.e., the allowance for being charged by plasma currents does not considerably affect the properties of screening.

Let us say a few words about the role of bound ionic states. In most of the literature, the effects related to the ions trapped by negatively charged grains are neglected. Nevertheless, it is *a priori* unclear to what extent the properties of screen-

ing can be affected by the presence of the bound states. An attempt to give some insight into this problem is made in references [14,19–22].

Strictly speaking, the relative contribution of bound states within the collisionless models is in principle indeterminate, which is, eventually, the consequence of the time-reversibility of Vlasov equation. The matter is that the stationary solutions of the Vlasov equation are dependent on the way the steady state of the system is formed. Thus, to tackle this problem, one has to employ additional considerations or principles in evaluating the number of the trapped ions.

As mentioned above, this problem was originally pointed out in the work [14]. The authors related the generation of bound states to the ion collisions. Recently, this idea was used while considering the presence of trapped ions in both analytical [21,22] and numerical [23] studies. These papers give answers to a number of important questions but many aspects of the problem still remain open. In particular, the bound ion distributions found in references [21,22] in the approximation of small collision frequency based on the calculations of free and bound ion balance, do not exhaust the variety of many other distributions which could exist in the absence of collisions.

The opposite case of strongly collisional plasma background is much less examined. In references [24–26] the grain screening has been studied based on the continuous drift-diffusion (DD) approximation. The effects of grain charging by plasma currents are essential in this case and the effective screened field considerably deviates from the predictions of DH theory. The main conclusion of the authors is that the effective potentials can be still fitted by DH theory, though, with effective parameters, and the screening length is, typically, longer than the Debye radius.

The goal of this paper is to give a concise review of further important results on the above issues recently obtained in [27–31].

2. Nonlinear phenomena in the grain screening and the structure of colloidal plasmas

In the case of thermodynamic equilibrium, an accurate description of nonlinear effects in grain screening can be obtained within the Poisson-Boltzmann (PB) approach describing the plasma as a two-component gas with Boltzmann distribution. The relevant equation for the case of a single spherical high- Z grain of a radius a in a plasma background reads

$$\Delta\varphi(r) = -4\pi en \left\{ \exp \left[-\frac{e\varphi(r)}{kT} \right] - \exp \left[\frac{e\varphi(r)}{kT} \right] \right\}, \quad (1)$$

with the boundary conditions for the effective self-consistent potential φ

$$\varphi'(a) = Ze/a^2, \quad \varphi(\infty) = 0,$$

specifying the electric field on the grain surface and the potential at infinity. Here e is the charge of a positively charged plasma particle and n is the plasma concentration at infinity.

The conventional treatment based on the assumption

$$\frac{e\varphi}{kT} \ll 1 \quad (2)$$

yields, after linearization with respect to φ , the well-known DLVO solution [6,7]

$$\varphi(r) = \frac{Z'e}{r} \exp\left(-\frac{r}{r_D}\right) \quad (3)$$

with the effective charge

$$Z' = Z \frac{\exp(a/r_D)}{1 + a/r_D}, \quad (4)$$

where r_D denotes the Debye screening length.

It is clear that at short distances the condition (2) is definitely violated. Thus, the transition $a \rightarrow 0$ with the DH limit

$$\varphi_D(r) = \frac{Ze}{r} \exp\left(-\frac{r}{r_D}\right) \quad (5)$$

is incorrect. In other words, in the case of a grain of a small size the nonlinear effects in screening may be significant and the applicability of equations (3,4) would break down.

To estimate the validity of the linear approximation, it is convenient to introduce the plasma-grain coupling

$$\chi = \frac{Ze^2}{kTa}$$

giving the potential-to-kinetic energy ratio for a plasma particle on the grain surface. As mentioned above, its magnitude for DP and CCS with high- Z impurities is of the order of $\simeq 10$, which casts doubt on the validity of the linear DH theory for the description of screening.

Below we consider the problem of screening of a finite-size charge Z in a plasma background for the range $\chi \simeq 1 - 50$ in two ways. The first one is the accurate numerical solution of the above PB equations. The other one is the method of MC computer simulations providing a microscopic description of screening.

The PB boundary problem (1) has been solved numerically, by using the shooting method and the second-order Runge-Cutta numerical algorithm [32]. The MC simulations of screening were performed for the NVT-ensemble using the conventional Metropolis algorithm [33], within the finite model with the microscopic two-component plasma background represented by a large number of charged hard spheres confined in a spherical volume with the grain fixed in the centre. The goal of computations was the effective screened potential $\varphi(r)$ and the charge distribution function $Q(r)$ defined as the ratio of the total charge residing within a sphere of a radius r to the grain charge.

Let us say a few words about the choice of parameters. The PB theory is based on the notion of the mean field, which loses its sense for strongly coupled plasma background, in the case that

$$\Gamma = \frac{e^2}{kTd} \geq 1,$$

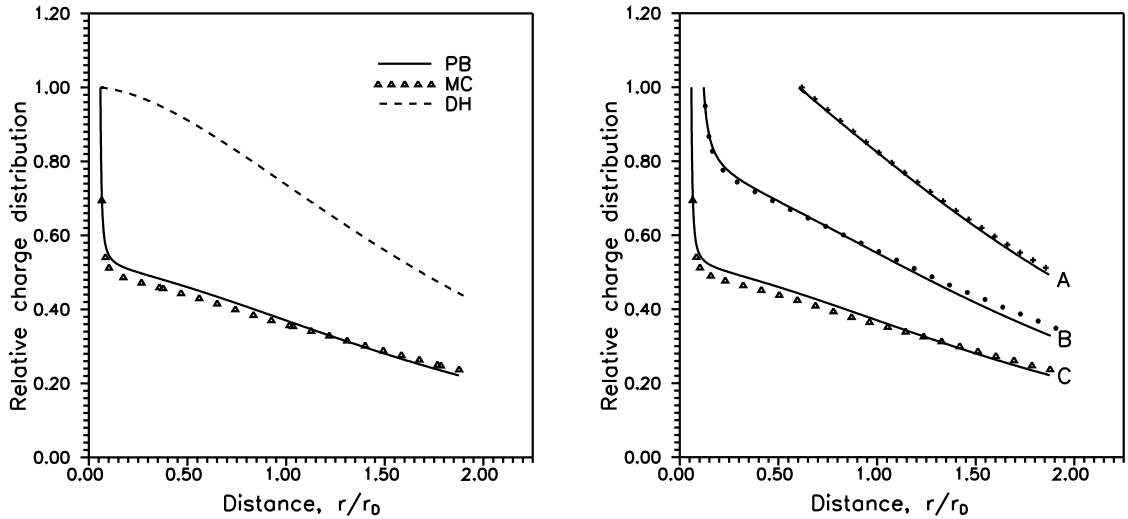


Figure 1. Comparison of the relative charge distributions near the charged grain obtained within the linear DH approximation (dashed line), nonlinear PB theory (solid line), and MC simulations (symbols) for $Z = 25$, $\Gamma = 0.1$. The plasma-grain coupling is $\chi = 20$ (left), and $\chi = 2$ (A), 10 (B), 20 (C) (right).

as the plasma correlations become significant. Here $d = (4\pi n)^{-1/3}$ is the average distance between plasma particles. Typical of CP are the values $Z \gg 1$, $\Gamma \ll 1$. Hereinafter we give the comparison of the results obtained within the two above approaches for $Z = 25$, $\Gamma = 0.1$ and 0.05 , $\chi = 2, 10, 20$.

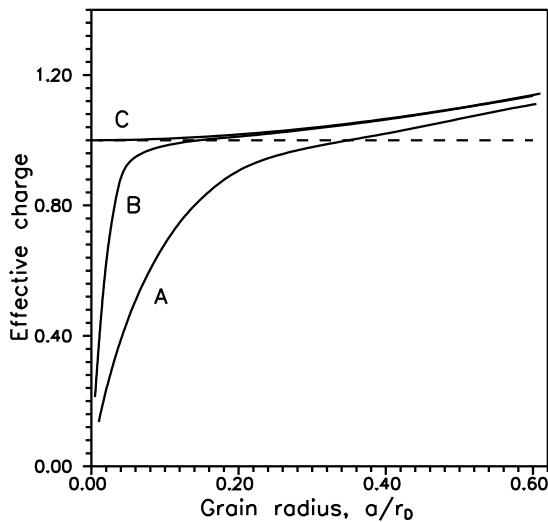


Figure 2. Relative effective charge Z^* vs. grain radius, determined as $Z^* = \varphi/\varphi_D$ at $r \gg a$; $Z = 25$, $\Gamma = 0.1$ (A), 0.05 (B). The line (C) corresponds to the linear DLVO approximation; the dashed line is the DH theory.

As follows from our computations, both approaches evidence (at strong plasma-grain coupling, and in a distinct contrast with the linear DH theory) the existence of an interesting effect connected with the accumulation of plasma charge on the grain surface (“plasma condensation”), which sharply affects the characteristics of screening, figures 1,2. While the asymptotic behavior of the screened potential at long distances retains its Yukawa-like form given by equation (5), the magnitude of the effective charge Z^* can be well described by the DLVO theory only for small χ . For stronger plasma-grain coupling, in a sharp contrast with the predictions of linear screening theory, the effective charge approaches zero, which evidences a pronounced enhancement of screening in this case.

An important point is the existence of a critical magnitude of this parameter, $\chi \simeq 4$ weakly depending on the other plasma parameters. It is interesting to note that this critical magnitude is much larger than unity, which means that the linear screening approximation is quite accurate even for the expansion parameter (2) ranging up to $\simeq 4 - 5$.

It is clear that the above phenomenon of nonlinear screening is of importance to the structural properties of CP. Its effect on the phase diagram for CCS can be illustrated based on the model of effective intergrain forces in the following way.

As mentioned above, the basic reference system of CP based on the notion of effective interaction is the Yukawa-system with the interparticle effective potential given by

$$\frac{V(x)}{k_B T} = \frac{\Gamma}{x} \exp\left(-\frac{x}{\Delta}\right), \quad (6)$$

with two dimensionless parameters: the coupling Γ and the screening length Δ ; x is the dimensionless distance.

Our study employs the connection between the dimensionless parameters Γ and Δ of a YS and the microscopic parameters of CP, which can be established as follows.

Let us consider a two-component asymmetric strongly coupled plasma, which is the simplest example of CP. Here a good microscopic model appears to be a system of charged hard spheres interacting through Coulomb forces. In case the size of a plasma particle is negligibly small (in agreement with physical situation in CP), such a system can be described by three dimensionless parameters, such as the packing fraction for the colloidal component

$$v = \frac{n\pi\sigma^3}{6},$$

the charge asymmetry Z , and the plasma-grain coupling χ .

Under the assumption that the screening of the grains is produced purely by plasma background and that the screening can be described in terms of the linear DH theory for point charges, one easily gets the effective interaction in the form (6), with the parameters of YS determined by

$$\Gamma = \frac{Z^2 e^2}{k_B T d}, \quad (7)$$

$$\Delta = r_D / d, \quad (8)$$

and the dimensionless distance specified as $x = r/d$. Here $d = (4\pi n_c)^{-1/3}$ is the average distance between colloidal plasma particles; $r_D = (4\pi n_{bg} e^2 / k_B T)^{-1/2}$ is the Debye screening length produced by the single plasma component.

Thus, the parameters entering the effective Yukawa interaction are expressed herewith via the microscopic plasma parameters. Our further considerations are based upon the idea that the properties of CP can be described by an effective pair interaction in the form (6) even in the case that the nonlinear screening is significant. As mentioned above and shown in [13], the effective screened potential retains in this case the Yukawa-like form at long distances. The effective charge,

however, should be found from the exact solution of the relevant PB equation; the background density n_{bg} , which determines the Debye length, is assumed to be equal to the average plasma background concentration. Within such an approach, the account of nonlinear effects reduces to re-scaling the well known melting curve for YS [9] with the use of the relevant *effective charge* Z^* instead of the *bare charge* Z . This latter can be evaluated by numerically solving the nonlinear PB equation for a single grain in one-component plasma background in a spherical cell with relevant parameters. An important point is that due to the connection between the microscopic parameters of two-component asymmetric plasmas and the parameters of the Yukawa model one can obtain important qualitative conclusions about a *minimal charge asymmetry* Z_{min} needed for the formation of Coulomb lattices in CP. Namely, there is a connection between the parameters Z , Γ and Δ :

$$Z = \Gamma \Delta^2, \quad (9)$$

which is the consequence of the relations (7), (8) and the global charge neutrality condition $Zn = n_{\text{bg}}$. Therefore, the parameter Z specified via equation (9), which has the physical meaning of charge asymmetry, can be used for the description of YS instead of coupling Γ . In other words, the relation (9) makes it possible to transfer the melting curves onto the $Z - \Delta$ plane.

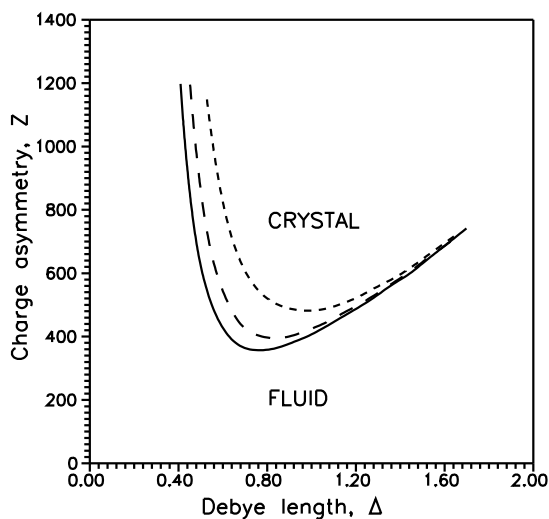


Figure 3. Melting curves for colloidal plasmas in $Z - \Delta$ plane. Solid line: $v = 5 \cdot 10^{-2}$; long dashes: $v = 5 \cdot 10^{-3}$; short dashes: $v = 5 \cdot 10^{-4}$. Nonlinear screening effects in shifting the melting curves to higher values of asymmetry Z at small packing fractions.

The results of computations of the melting curves are given in figure 3. As can be seen, there exists a minimal charge asymmetry $Z_{\text{min}} = 355$ needed in order to obtain a crystal state. The same conclusion and a close value of $Z_{\text{min}} = 360$ was obtained in [34] based on the Lindemann melting criterion for the case of specific effective grain-grain forces. The lower melting curve in the figure 3 is close to that given in that work. However, we see that the allowance for the nonlinear screening results in shifting the melting curves to higher values of charge asymmetry Z at small packing fractions of a colloidal component.

It should be noted that our considerations are based on the effective Yukawa interaction in the form (6) which is expected to work in the case of dilute charged colloidal suspensions with high charge asymmetry and weakly coupled plasma background [35]. The effects of nonlinear background screening are commonly accepted to be associated with induced many-body forces between colloidal

particles and are expected to become relevant for moderate packing fractions. The present example shows that the nonlinear screening may be important in the case of small packing fractions as well.

A more accurate description of the structure of CP can be obtained by means of MC computer simulations based on the microscopic model of asymmetric two-component plasmas (TCP). As shown above, the nonlinear grain screening obtained within PB theory has the direct analogue in the MC simulations with the microscopic description of plasma background, i.e., the phenomenon of “plasma condensation” near the grain surface. This suggests that the above phenomenon should manifest itself in MC simulations of asymmetric TCP affecting its structural properties as well.

Below we give our results of MC simulations of strongly coupled TCP with the charge asymmetry up to $Z = 100$ based on the “primitive model” aimed at the elucidation of the nonlinear effects on the structural properties of TCP.

Within the “primitive” model, a TCP is considered as an overall charge neutral mixture of charged spherical grains in a compensating plasma background. In all the simulations we assume the size of a plasma particle to be negligibly small, in accord with the physical situation in CP. We performed MC simulations of such a system for canonical ensemble by using the conventional Metropolis algorithm and periodic boundary conditions [33]. An accurate account of long-range Coulomb forces was achieved due to Ewald’s summation procedure [36].

The idea of simulations was to study radial grain-grain and plasma-plasma distributions near the critical point $\chi \simeq 4$. In particular, we performed a number of simulations for different values of plasma-grain coupling χ though for a fixed value of coupling $\Gamma_c = Z^2 e^2 / k_B T d_c$ in the colloidal component (we use here a slightly different definition for the average interparticle distance $d_c = (4\pi n_c / 3)^{-1/3}$). The range of parameters was as follows: the charge asymmetry $Z = 10 - 100$, volume fractions of colloidal component $v_c = 0.001 - 0.1$, the coupling $\chi = 1 - 50$. Note that these parameters are connected with the coupling Γ_c by the relation

$$\Gamma_c = Z\chi v_c^{1/3}. \quad (10)$$

Therefore, by varying the charge asymmetry Z of a TCP, one can change the parameter χ while holding the above coupling Γ_c constant.

The results for $Z = 10; 15; 24; 60; v_c = 0.01; \chi = 2 - 40$ are presented in the figures. The most remarkable result consists in a pronounced change in the behavior of the system near the point $\chi \simeq 4$. If the coupling between the components χ is smaller than 4, the TCP grain-grain distribution exhibits an oscillatory behavior characteristic of a liquid phase. It means that the effects of screening produced by the plasma component, do not qualitatively change the properties of the colloidal component, and the latter behaves like one-component plasma. In figure 4, we can see that in this case (for $\chi = 2$ and 3) the plasma-plasma distributions are characteristic of a gas phase. In the case of strong plasma-grain coupling $\chi > 4$ the reduction in grain-grain correlations, and the appearance of correlations (on the length of the order of the grain diameter σ_c) in plasma-plasma distributions are

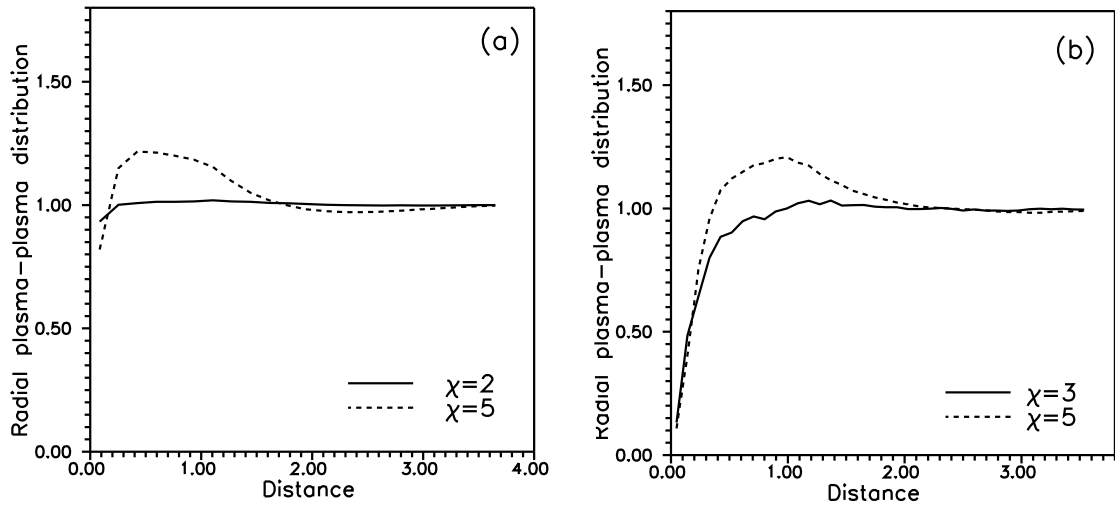


Figure 4. Radial plasma-plasma distribution functions for infinite TCP: (a) $\Gamma_c = 26$, $v_c = 0.01$. Solid line: $\chi = 2$, $Z = 60$. Dashed line: $\chi = 5$, $Z = 24$. (b) $Z = 10$, $v_c = 0.01$. Solid line: $\chi = 3$, $\Gamma_c = 6.5$. Dashed line: $\chi = 5$, $\Gamma_c = 10.8$. The unit of distance is σ_c .

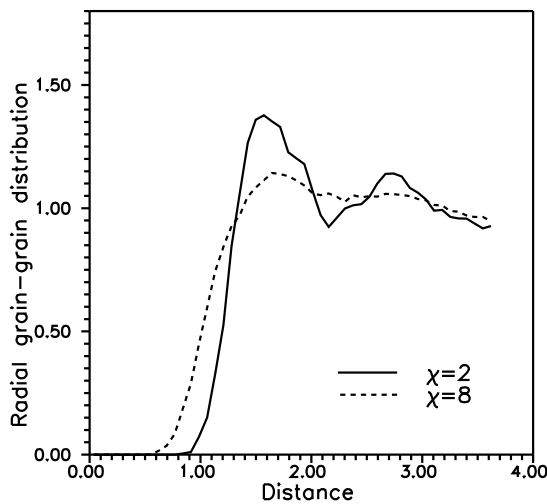


Figure 5. Radial grain-grain distribution functions for infinite TCP for the same grain-grain coupling $\Gamma = 26$ and packing fraction $v_c = 0.01$ (liquid state). Solid line: $\chi = 2$; dashed line: $\chi = 8$; the charge asymmetry $Z = 60$ and 15. The unit of distance is d_c .

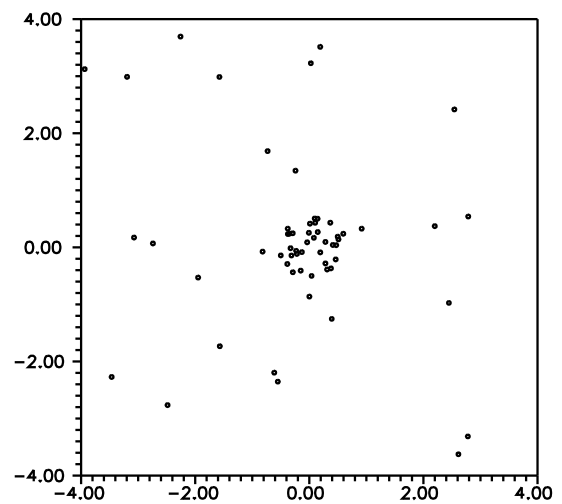


Figure 6. Equilibrium configuration for the plasma component near a single grain, $Z = 100$; the coupling in the plasma background is $\Gamma_p = 0.05$; $\chi = 20$. The unit of distance is σ_c .

observed, figures 4, 5. These indicate a pronounced enhancement of grain screening and the accumulation of plasma particles near grain surfaces. Remarkably, this was observed in all the simulations near the same threshold value $\chi = 4$ within a wide range of other parameters of TCP regardless of the way of simulations. Direct visual observations of equilibrium configurations for strong plasma-grain coupling also evidence the accumulation of plasma particles near the grains, figure 6.

Thus, we see that the qualitative change in the structural properties near the point $\chi = 4$ is a rather general feature of asymmetric TCP and the threshold value obtained in MC simulations of this system is in a good agreement with the studies of nonlinear screening of a single grain based on the continuous PB theory.

3. Grain screening in collisionless plasmas and the effects of trapped ions

As mentioned in the introduction, the problem of grain screening in collisionless background with regard to the effect of plasma particle loss at the grain surface has attracted much attention of the researchers. However, the effects of trapped ions remain in many respects poorly known.

The purpose of this section is an attempt to elucidate the properties and the role of bound ionic states in grain screening within the nonlinear collisionless model in the case of a grain charged by plasma currents. In particular, we are going to focus on the effects produced by various numbers of trapped ions on the charge densities and the effective screened potentials.

We start from the conventional Poisson equation for a single charged spherical grain of a radius a immersed in a plasma background

$$\Delta\phi(r) = -4\pi e[Z_i n_i(r) - n_e(r)] \quad (11)$$

with the ion and electron densities $n_i(r)$ and $n_e(r)$ being specified as

$$n_i(r) = n_{ib}(r) + n_{if}(r),$$

where

$$\begin{aligned} n_{if}(r) = & \frac{n_{0i}}{2} \exp\left[-\frac{Z_i e \phi(r)}{k_B T_i}\right] \left\{ 1 - \operatorname{erf}\left(\frac{v_{ib}}{\sqrt{2}s_i}\right) + \frac{2}{\sqrt{\pi}} \frac{v_{ib}}{\sqrt{2}s_i} \exp\left(-\frac{v_{ib}^2}{2s_i^2}\right) \right. \\ & + \sqrt{1 - \frac{a^2}{r^2}} \exp\left(-\frac{v_{imin}^2}{2s_i^2}\right) \left[1 - \left(\operatorname{erf}\left(\frac{\sqrt{v_{ib}^2 - v_{imin}^2}}{\sqrt{2}s_i}\right) \right. \right. \\ & \left. \left. - \frac{2}{\sqrt{\pi}} \frac{\sqrt{v_{ib}^2 - v_{imin}^2}}{\sqrt{2}s_i} \exp\left(-\frac{v_{ib}^2 - v_{imin}^2}{2s_i^2}\right) \right) \theta(v_{ib}^2 - v_{imin}^2) \right] \right\}, \quad (12) \end{aligned}$$

$$\begin{aligned} n_{ib}(r) = & \mathcal{A} n_{0i} \exp\left[-\frac{Z_i e \phi(r)}{k_B T_i}\right] \sqrt{1 - \frac{a^2}{r^2}} \exp\left(-\frac{v_{imin}^2}{2s_i^2}\right) \\ & \times \left[\operatorname{erf}\left(\frac{\sqrt{v_{ib}^2 - v_{imin}^2}}{\sqrt{2}s_i}\right) - \frac{2}{\sqrt{\pi}} \frac{\sqrt{v_{ib}^2 - v_{imin}^2}}{\sqrt{2}s_i} \exp\left(-\frac{v_{ib}^2 - v_{imin}^2}{2s_i^2}\right) \right] \theta(v_{ib}^2 - v_{imin}^2), \quad (13) \end{aligned}$$

and

$$\begin{aligned}
 n_e(r) = & \frac{n_{0e}}{2} \exp\left[\frac{e\phi(r)}{k_B T_e}\right] \left\{ 1 + \operatorname{erf}\left(\frac{v_{e0}}{\sqrt{2}s_e}\right) - \sqrt{\frac{2}{\pi}} \frac{v_{e0}}{s_e} \exp\left(-\frac{v_{e0}^2}{2s_e^2}\right) \right. \\
 & + \sqrt{1 - \frac{a^2}{r^2}} \exp\left(\frac{v_{e0}^2}{2s_e^2} \frac{a^2}{r^2 - a^2}\right) \left[1 - \operatorname{erf}\left(\frac{v_{e0}}{\sqrt{2}s_e} \sqrt{\frac{r^2}{r^2 - a^2}}\right) \right. \\
 & \left. \left. + \sqrt{\frac{2}{\pi}} \frac{v_{e0}}{s_e} \sqrt{\frac{r^2}{r^2 - a^2}} \exp\left(-\frac{v_{e0}^2}{2s_e^2} \frac{r^2}{r^2 - a^2}\right) \right] \right\}. \quad (14)
 \end{aligned}$$

Here $n_{ib/if}(r)$ is the density of bound/free ions, $n_{0i/0e}$ is the ion/electron density at infinity; $\phi(r)$ is the self-consistent effective potential; e is the absolute value of the electron charge; $T_{i/e}$ is the ion/electron temperature; $s_{i/e} = \sqrt{k_B T_{i/e}/m_{i/e}}$ is the thermal ion/electron velocity; $m_{i/e}$ is the ion/electron mass, and Z_i is the ion charge number.

Also, here we introduced the notation

$$\begin{aligned}
 v_{i0}^2 &= \frac{2eZ_i}{m_i} [|\phi(a)| + \phi(r)], & v_{ib}^2 &= \frac{2eZ_i}{m_i} |\phi(r)|, \\
 v_{imin}^2 &= \frac{a^2 v_{i0}^2}{r^2 - a^2}, & v_{e0}^2 &= \frac{2e}{m_e} [|\phi(a)| + \phi(r)].
 \end{aligned}$$

The relations (12)–(14) can be obtained by integrating the Maxwellian distributions over velocities taking into account the energy and angular momentum conservation laws and the limitations imposed by the presence of the absorbing grain. I.e., i) we take into account all the ion and electron trajectories which do not touch the grain, ii) we exclude from the phase space all the finite ion trajectories which intersect the grain surface, and iii) we exclude the outgoing free ion or electron trajectories, which previously met the grain. Notice that the above equations also follow from the stationary solution of the Vlasov equation with the appropriate boundary conditions (Maxwellian distributions at the infinity and zero value of distribution functions with positive radial velocity at the grain surface).

It should be noted that in the derivation of the density for bound ions, we also start from the Maxwellian distribution, though the finite trajectories do not reach the infinity and, therefore, cannot be coupled to the heatbath. Thus, we employ an additional assumption that the bound states are initially formed with equilibrium distribution.

The relation (13) contains a free parameter, the amplitude \mathcal{A} , which determines the relative contribution of bound ionic states to the charge density. As mentioned in the Introduction, its value is indeterminate within the collisionless model, because the concentration of bound states cannot be related in any way to the ion concentration at infinity. However, some reasonable estimates for the magnitude of \mathcal{A} can be obtained as follows. Consider the limit $a \rightarrow 0$ in equations (12)–(14). It can be verified that the value $\mathcal{A} = 1$ can be found from the additional requirement for the distributions to be Boltzmannian, which corresponds to the case of thermodynamic

equilibrium. It is natural to assume that, in general case, the value of \mathcal{A} , though being dependent on various physical situations (i.e., on how the system reaches its steady state), would have a magnitude of the same order.

In order to solve the problem (11)–(14) within the interval $a \leq r \leq r_{\max}$, we have to formulate the boundary conditions for the effective potential $\phi(r)$

$$\phi(a) = \phi_0, \quad (15)$$

$$\phi(r_{\max}) = \phi_{\text{as}}. \quad (16)$$

Here, the right boundary r_{\max} has to be chosen at a sufficiently long distance, $r_{\max} \gg r_D$, so that the potential is described by its asymptotic value ϕ_{as} . The latter is known [17,18], and it reads

$$\begin{aligned} \phi_{\text{as}}(r) &\simeq -\pi en_{0i} a^2 \left(1 + \frac{2eZ_i |\phi_0|}{k_B T_i} \right) \frac{r_D^2}{r^2} \\ &= -\frac{T_e}{2Z_i(T_e + T_i)} \left(Z_i + \frac{k_B T_i}{2e|\phi_0|} \right) \frac{a^2}{r^2} |\phi_0|. \end{aligned} \quad (17)$$

The boundary value of the potential ϕ_0 at the grain surface is determined by the balance of plasma currents to the grain surface. In order to find it, we use the well-known equation [37]

$$\frac{\omega_{pe}^2}{s_e} e^{-u} = \frac{\omega_{pi}^2}{s_i} (t + u). \quad (18)$$

Here $\omega_{p\sigma}^2 = 4\pi e_\sigma^2 n_\sigma / m_\sigma$, $s_\sigma = (k_B T_\sigma / m_\sigma)^{1/2}$, $t = T_i / T_e Z_i$, n_σ is the particle density of σ species at infinity, and $u = e|\phi_0| / k_B T_e$ is the sought-for dimensionless potential at the grain surface.

The two-point boundary value problem for the effective potential (11)–(16) was solved numerically by using the shooting methods [32]. The computations were performed for the following range of parameters: $\tau = T_i / T_e = 0.08 - 1.0$, $\rho = a / r_D = 0.015 - 3.0$, $\mathcal{A} = 0 - 10$, $Z_i = 1$, $\mu = m_i / m_e = 10^4$.

The results of computations are given in the figures.

In figure 7 the behavior of plasma charge densities associated with the calculated effective potentials are displayed within a typical range of parameters. As is seen, the bound ionic states tend to concentrate in the vicinity of the grain surface. The most remarkable feature in the behavior of the bound ion states is that, beginning with some critical distance r_c , the density of bound states is strictly equal to zero. In figure 8 we give the relevant dependencies for r_c obtained in our calculations. Notice that, with the increasing the grain size, the value r_c diminishes. As a result, in the case of very large grains, for $a \simeq 2 - 3r_D$, the bound states cannot exist at all. This conclusion is in agreement with the results of reference [14], where it was mentioned that the role of the bound states for large grain sizes is insignificant.

Let us show that this effect is connected with the asymptotic behavior of the effective potential inversely proportional to the square distance. The expression for the density of the bound states (13) contains a multiplier, θ -function accounting for

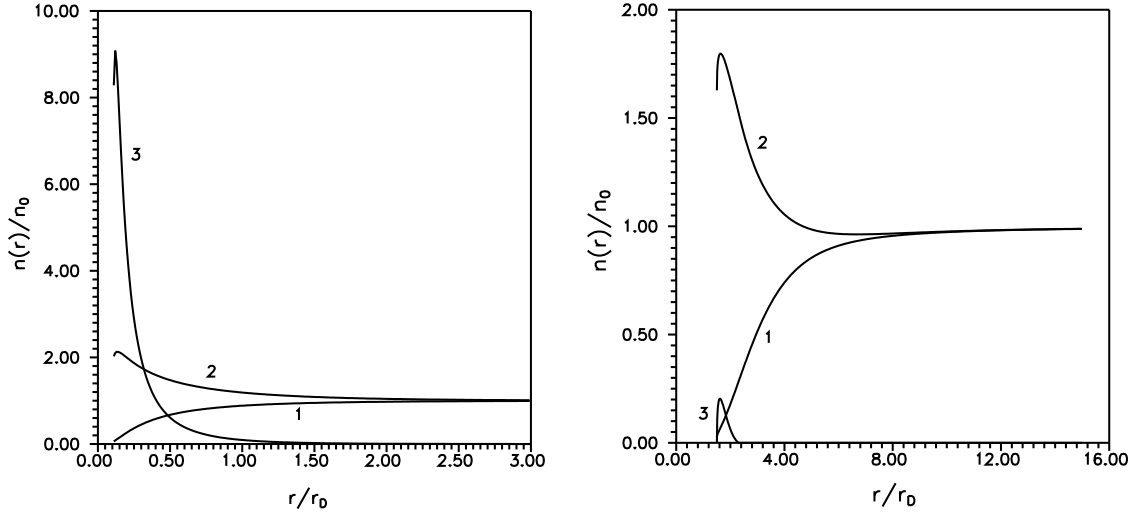


Figure 7. Charge densities for electrons (1), free (2) and bound (3) ionic states vs. distance for $\tau = 0.4$, $\mathcal{A} = 1.0$, $\rho = 0.1$ (left), and $\rho = 1.5$ (right).

the loss of ions with the trajectories meeting the grain. Its argument is given by

$$\eta = v_{\text{ib}}^2 - v_{\text{imin}}^2 = \frac{2eZ_i}{m_i(1 - a^2/r^2)} \left\{ |\phi(r)| - \frac{a^2}{r^2} |\phi(a)| \right\}.$$

At larger distances, the potential $\phi(r)$ may be replaced by its asymptotic expression (17). In this case, the argument of the θ -function

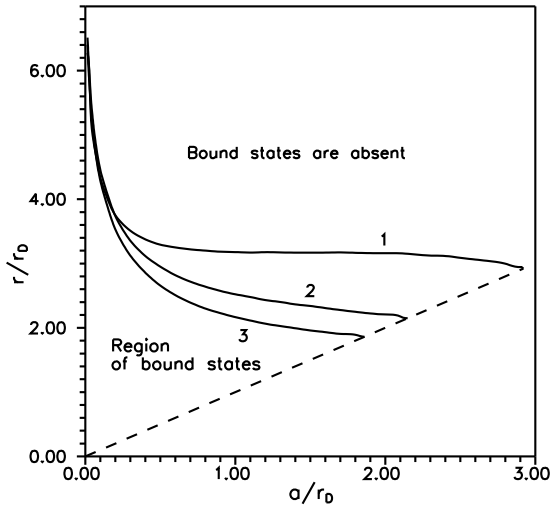


Figure 8. Critical distance r_c (dividing the region with bound ionic states and the region where they are absent) vs. the grain radius for $\tau = 0.08$ (1), 0.4 (2), 1.0 (3). The amplitude $\mathcal{A} = 1.0$.

$$\eta(r \rightarrow \infty) = - \left[1 + 2\tau \left(1 - \frac{1}{4Z_i u} \right) \right] \times \frac{a^2 |\phi_0|}{r^2} \frac{eZ_i}{m_i(1 - a^2/r^2)(1 + \tau)}$$

is always negative, $\eta(\infty) < 0$, since $Z_i \geq 1$ and $u = e|\phi_0|/k_B T_e \geq 1$. It means that the density of the bound states is equal to zero (i.e. they are absent) at larger distances, where the potential assumes its asymptotic form.

In figure 9 the calculated effective potentials are displayed. As can be seen, the allowance for the bound ionic states for the amplitudes $\mathcal{A} = 0 - 1$ results in rather insignificant changes in effective potentials, suggesting that the densities of free and bound ions adjust themselves self-consistently to produce very close potentials for different values of \mathcal{A} .

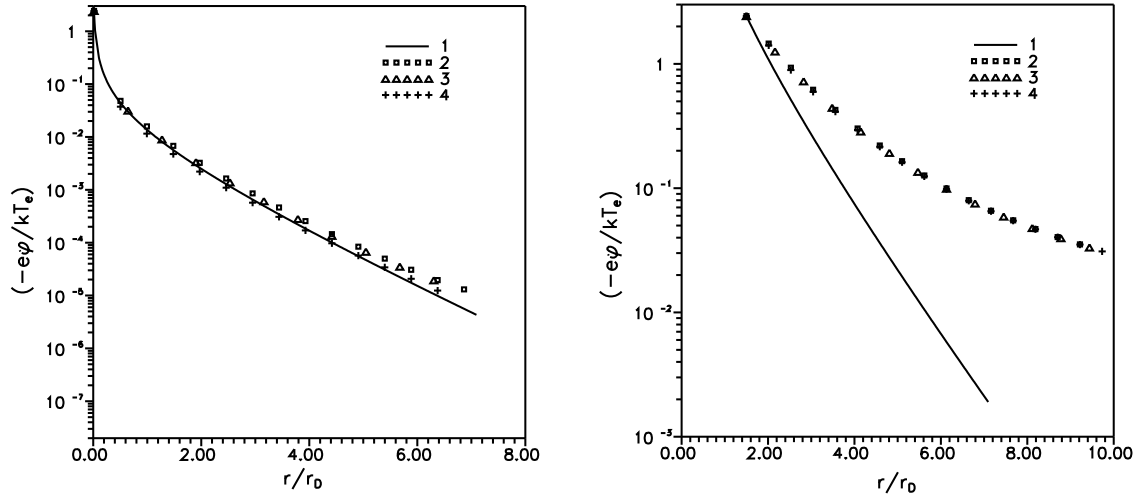


Figure 9. Comparison of the DH theory (1) with the calculated effective potentials for $\mathcal{A} = 0$ (2), 0.1 (3), 1.0 (4). The ion-to-electron temperature ratio is $\tau = 0.08$, the grain radius is $\rho = 0.015$ (left) and $\rho = 1.5$ (right).

Remarkably, for smaller grain sizes, $a \simeq 0.01r_D$, the critical radius r_c tends to increase indicating that the region where the potential takes its asymptotic form moves to larger distances. In this case, the effective potentials within the region $r < r_c$ are very close to those predicted by DH theory. This conclusion is in agreement with the theoretical results of the papers [16,20], as well as with the recent experiments [38], where the Yukawa type of the effective grain-grain interactions was demonstrated in the direct measurements.

4. Screening of a grain charged by plasma currents in strongly collisional background

In this section we consider the screening of a spherical grain charged by plasma currents in a weakly ionized high pressure gas. As will be shown below, the properties of grain screening in this case substantially depend on the type of boundary conditions (BC). In contrast to the works [24–26], where complicated semirealistic multigrain systems with relevant specific BC are considered, we are going to examine the simplest case of a *single* grain with the emphasis on the basic features of this problem.

Thus, we examine a single spherical grain of a radius a imbedded in a weakly ionized high pressure gas. In this case, it is natural to use the drift-diffusion (DD) approach, because the collisions of plasma particles with the neutrals play here a dominant role. Assuming two types of plasma particles (ions and electrons) only, we write the general time-dependent equations for the unknown ion/electron densities $n_{i,e}$ and self-consistent potential ϕ in the form

$$\frac{\partial n_{i,e}}{\partial t} = -\text{div}\mathbf{j}_{i,e} + I_0 - \alpha n_i n_e, \quad (19)$$

$$\Delta\phi = -4\pi e(n_i - n_e). \quad (20)$$

Here, α is the coefficient of recombination, I_0 is the intensity of plasma ionization (we examine the case of uniformly distributed plasma sources). The expression for the current densities $\mathbf{j}_{i,e}$ is as follows:

$$\mathbf{j}_{i,e} = -\mu_{i,e}n_{i,e}\nabla\phi - D_{i,e}\nabla n_{i,e},$$

where $\mu_{i,e}$ and $D_{i,e}$ are the ionic/electronic mobility and diffusivity, respectively. These latter are assumed to be related by the Einstein's equation $\mu_{i,e} = z_{i,e}e_{i,e}D_{i,e}/k_B T$ (here $z_{i,e} = \pm 1$ is the ion/electron charge number). In a weakly ionized gas with dominating plasma-neutrals collisions, it is reasonable to assume that the ion and electron temperatures are equal. Thus, hereinafter we consider only the case that $T_i = T_e = T$. The grain charge emerges as a result of plasma currents due to the difference in electron and ion diffusivities. With regard to spherical symmetry, the relevant equation for the grain charge number Z reads

$$\frac{dZ}{dt} = -4\pi a^2(j_{(r)i} - j_{(r)e}), \quad (21)$$

where the subscript (r) denotes the radial component of a current.

In order to formulate the BC, we admit that the system is confined within a spherical volume of sufficiently large radius $R \simeq 50 - 500r_D$ (where r_D is the Debye screening length) with the grain placed at the center. The BC are specified at the surface of this sphere and at the surface of the grain. In our simulations, we consider the two basic cases and two types of BC, respectively. In the first case (I), the sources of plasma ionization, which compensate the losses of plasma particles due to the absorption on the grain surface, are assumed to be far from the grain (outside the spherical volume). The action of these sources is modelled by maintaining constant electron and ion densities on the surface of the sphere, $n_i = n_e = n_0$. According to this, we write the BC for the densities $n_{i,e}$

$$n_{i,e} = n_0, \quad r = R,$$

and assume the rates of plasma ionization and recombination over the volume I_0 and α to be equal to zero. In the second case (II), we examine the problem with uniformly distributed plasma sources ($I_0 \neq 0$) with allowance for the plasma recombination over the volume ($\alpha \neq 0$). Note, that in this case the quantities I_0 and α are related to the unperturbed bulk plasma density n_0 by the equation $I_0 = \alpha n_0^2$ valid in the absence of the grain. The relevant BC read

$$\frac{\partial n_e}{\partial r} = \frac{\partial n_i}{\partial r} = 0, \quad r = R.$$

The BC for the potential at the grain surface have the form

$$\frac{\partial\phi}{\partial r} = -\frac{Z(t)e}{a^2}, \quad r = a$$

and for the densities $n_{i,e}$ we use the BC [24]

$$n_{i,e} = 0, \quad r = a$$

appropriate for the case of strongly collisional background.

We solved the above system of equations (19)–(21) using the method of lines and the Gear’s method. In addition, we performed a limited number of Brownian dynamics (BD) simulations based on the particle-in-cell (PIC) method [39] with spherically symmetric concentric cells and the BC corresponding to the case (I). In these simulations, the plasma background is modelled by finite numbers of particles of two types representing the ion and the electron components. The dynamics of the system is governed by the reduced Langevin equations of overdamped motion

$$h \frac{d\mathbf{x}_k}{dt} = -\nabla_k U + \mathbf{F}_k(t).$$

Here, \mathbf{x}_k is the radius vector of the k -th particle, and U is the potential energy of the configuration. The friction coefficient h and the random force $\mathbf{F}_k(t)$ are determined by the properties of the heatbath (in our case the role of the heatbath is played by the high pressure neutral gas). Random force acting on k -th particle is specified by the Gaussian distribution

$$P(\mathbf{B}_k(\Delta t)) = \frac{1}{(4\pi h^2 D \Delta t)^{3/2}} \exp \left[-\frac{|\mathbf{B}_k(\Delta t)|^2}{4h^2 D \Delta t} \right],$$

which determines the probability for the momentum

$$\mathbf{B}_k(\Delta t) = \int_t^{t+\Delta t} \mathbf{F}_k(t) dt$$

to be transferred to the k -th plasma particle during the time span Δt . The random forces, which act on different plasma particles are uncorrelated. It is clear that the quantities h and D related to the ion and the electron components are different. In the above expressions, we omitted the subscripts for simplicity. Note that the friction coefficient h can be expressed via diffusivity and temperature, $hD = k_B T$, which enables one to establish the correspondence with the continuous DD approach. A detailed presentation of the issues concerning BD and its relation to the continuous probabilistic approaches, such as Fokker-Planck and Smolukhovsky equations, can be found in references [40,41]. Here we would like to point out that the overdamped BD represents the direct microscopic analogue to the DD approach, since the latter can be derived from the Smolukhovsky equations for one-particle distributions (i.e., within the additional mean field approximation). The aim of BD simulations was to test the results of the DD approximation.

The range of parameters is typical of the DP experiments in high pressure weakly ionized noble gases like Ne or Ar: plasma background coupling $\Gamma \simeq 10^{-3}$; plasma density $n_0 \simeq 10^{10} \text{ cm}^{-3}$; the density of the neutrals $n \simeq 10^{18} \text{ cm}^{-3}$; radius of the grain $a \simeq 10^{-3} \text{ cm}$; electron-ion recombination coefficient $\alpha \simeq 10^{-7} \text{ cm}^3/\text{sec}$; the ratio of

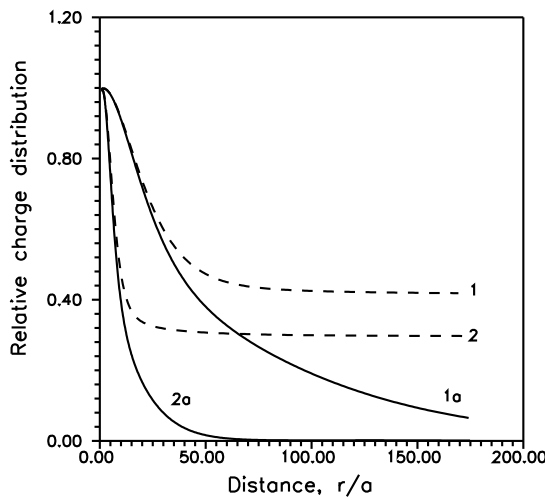


Figure 10. Comparison of charge distributions for different types of BC for the same stationary bulk plasma parameters. The Debye length is $r_D/a = 10$ for (1) and (1a), and $r_D/a = 2$ for (2) and (2a). Dashed and solid lines relate to the BC (I) and (II), respectively.

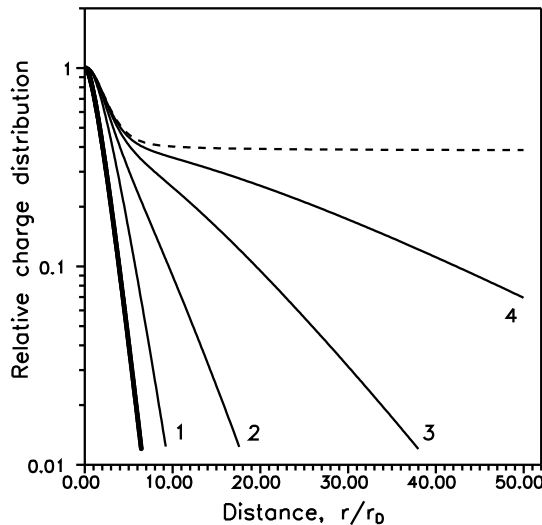


Figure 11. Relative charge distributions as dependent on the ionization rates for BC (II) at a fixed bulk plasma density. The dimensionless intensity of plasma sources over the volume $i_0 = I_0 a^5 / D_i$ is (1) $1.25 \cdot 10^{-2}$, (2) $2.5 \cdot 10^{-3}$, (3) $5 \cdot 10^{-4}$, (4) 10^{-4} . The bold line relates to the linear DH theory; dashed line is DD approach for BC (I). The grain radius a/r_D is 0.158.

the Debye length to the grain radius $r_D/a \simeq 0.1 - 50$. The ratio of diffusivities in all computations was fixed, $A = D_e/D_i = 10^3$ (with the exception for the BD simulations). The goal of the simulations was the final time-independent density and charge distributions which establish themselves after sufficiently long period of relaxation.

The results of computations are given in the figures. In figure 10, we give the relative charge distributions for different types of BC. Remarkably, in the case of BC (I), we observe the Coulomb-type asymptotic behavior of the screened field with the effective charge determined by the asymptotic value of the charge distribution. Note that such an asymptotic behavior of the screened field may be viewed as a consequence of the Ohm's law for the problem under consideration. In contrast to the case (I), the screening in the case of ionization over the volume has a finite screening length $\simeq 10 - 50r_D$. The computations performed for the same plasma parameters, in particular, for the same steady bulk density n_0 at long distances for the cases (I) and (II) indicate that there exist a sheath ranging up to $10r_D$ independent of the type of BC (provided that the ionization rate is relatively low). At longer distances, a distinct difference in the asymptotic behavior is observed. The stationary grain charges acquired by the grain in both cases are nearly equal.

Figure 11 illustrates the behavior of the relative charge distributions as dependent on the rate of ionization. The bulk plasma density is held constant therewith due to the simultane-

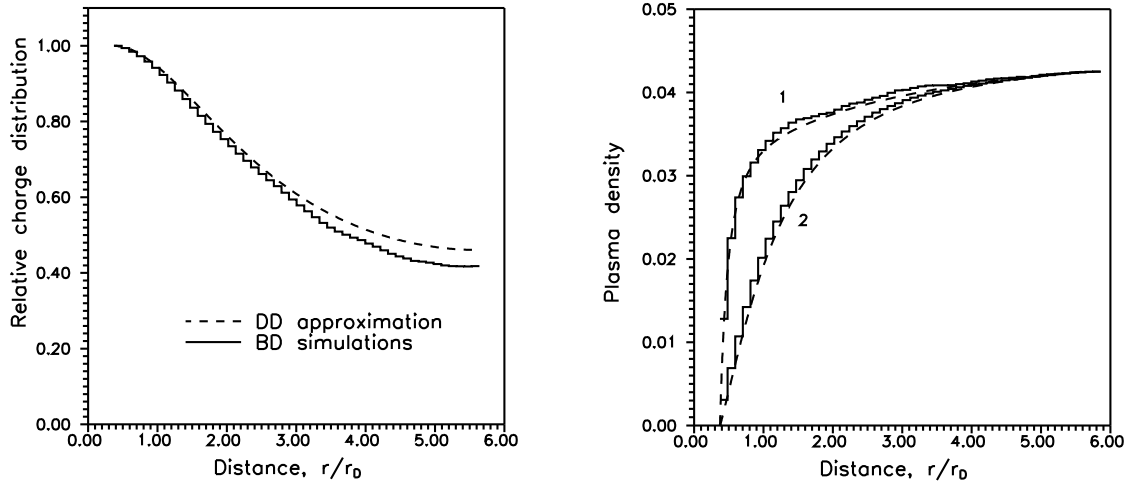


Figure 12. Comparison of the results of DD and BD simulations for the same parameters, $a/r_D = 0.373$, $A = 10.0$. Left: relative charge distributions. Right: comparison of ion (1) and electron (2) densities obtained in DD approximation (dashed lines) and in BD simulations (solid lines).

ous appropriate change of the recombination coefficients. The approximate straightness of the lines outside the sheath (on the log scale) suggests the exponential type of the screening at distances. Different rates of ionization (and recombination) correspond to the different slopes and the screening lengths, respectively. The higher is the intensity of ionization, the shorter is the length of screening. At higher rates, the relative indifference of the sheath is likely to break down, and the properties of screening approach the predictions of the DH theory (the bold line in figure 11). We see that, typically, the charging plasma currents in the presence of collisions result in the increase of the length of screening, as compared to the equilibrium DH theory. These results correlate qualitatively with those of reference [26] dealing with a more complicated case of non-isothermic nitrogen plasma.

Comparison of the continuous DD approach and the microscopic BD simulations shows a qualitative agreement between both cases, see figure 12. Some discrepancy (DD approach yields approximately 10% higher absolute value of the stationary grain charge) is, apparently, the result of microscopic effects in the plasma background in BD simulations.

5. Conclusions

Thus, we see that the properties of screening of high- Z impurities in colloidal plasmas may considerably vary depending on the physical processes in the plasma background.

The nonlinear effects in screening in the thermodynamically equilibrium case of a high- Z grain with a fixed charge (e.g., the case of colloidal suspensions) are essential for a strong plasma-grain coupling. The nonlinearity is associated with the accumulation of plasma particles on the grain surface and results in a sharp decrease

of the effective charge as compared with the linear theory. The linear DLVO theory works well only for weak plasma-grain coupling, $\chi < 4$. The nonlinear effects have a number of consequences for the structural properties of strongly coupled CP. In particular, they give rise to qualitative changes in the pair distribution functions and result in shifting the melting curves to larger magnitudes of charge asymmetry.

The grain screening in the collisionless background, with regard to the absorption of plasma particles by the grain, is close to the predictions of the DH theory (in the vicinity of grains) for the range of plasma parameters typical of DP and for small grain sizes ($a \ll r_{\text{Deb}}$). At longer distances, we observe the asymptotic behavior of the effective potentials inversely proportional to the squared distance. The bound ionic states result in considerable changes in the plasma densities near the grain. However, they weakly affect the effective potentials in these conditions. The presence of the bound states is limited by some critical distance ($\simeq 2 - 3r_{\text{Deb}}$), beyond which they cannot exist at all.

The processes of grain charging in strongly collisional plasma background result in a considerable deviation from the equilibrium DH theory. In case the plasma sources are placed at infinity, at long distances we observe the Coulomb field with a certain effective charge. The effect of screening manifests itself in the decrease of this effective charge as compared to the stationary grain charge. The smaller is the ratio of the Debye length to the grain size, the smaller effective charge is observed. In case the plasma sources are distributed uniformly over the volume, there exists a finite screening length depending on the rate of ionization. Typically, this screening length in the presence of plasma currents and strong collisions considerably exceeds the Debye radius. The stationary grain charge as well as the field within the sheath around the grain ($\simeq 10r_{\text{D}}$) does not depend on the type of BC and on the ionization rate, provided that this latter is relatively low. At higher ionization rates, the properties of screening approach the predictions of DH theory.

In conclusion, we would like to mention that an important problem, which still remains poorly examined, is the properties of grain screening in a weakly collisional and intermediate case. It would be interesting to study this issue within the Bhatnagar-Gross-Krook model, or based on the Fokker-Planck equations. Of particular interest is the collisionless limit obtained within these approaches, which could be compared to the results of the paper [21]. Further valuable information on the above issues could be obtained by means of microscopic computer simulations in the spirit of reference [23].

References

1. Thomas H., Morfill G.E., Demmel V., Goree J., Feuerbacher B., Möhlmann D. // Phys. Rev. Lett., 1994, vol. 73, p. 652.
2. Chu J.H., Lin I. // Physica, 1994, vol. A205, p. 183.
3. Tsytoich V.N. // Phys. Usp., 1997, vol. 40, p. 53.
4. Pieransky P. // Contemp. Phys., 1983, vol. 24, p. 25.
5. Löwen H. // Phys. Rep., 1994, vol. 237, No. 5, p. 249.

6. Derjaguin B.V., Landau L. // *Acta Physicochimica (USSR)*, 1941, vol. 14, p. 633.
7. Verwey E.J., Overbeek J.Th.G. *Theory of the Stability of Lyophobic Colloids*. Elsevier, Amsterdam, 1948.
8. Meijer E.J., Frenkel D. // *J. Chem. Phys.*, 1991, vol. 94, p. 2269.
9. Robbins M.O., Kremer K., Grest G. S. // *J. Chem. Phys.*, 1988, vol. 88, p. 286.
10. Dupont G. et al. // *Mol. Phys.*, 1993, vol. 79, p. 453.
11. Fortov V.E., Yakubov I.T. *Physics of Nonideal Plasmas*. New York, Hemisphere, 1992.
12. Xu Y., Chen Y.-P. // *Phys. Scripta*, 1999, vol. 60, p. 176.
13. Alexander S., Chaikin P.M., Grant P., Morales G.J., Pincus P. // *J. Chem. Phys.*, 1984, vol. 80, p. 5776.
14. Bernstein I.B., Rabinovitz I.V. // *Phys. Fluids*, 1959, vol. 2, p. 112.
15. Laframboise J.G., Parker L.W. // *Phys. Fluids*, 1973, vol. 15, p. 629.
16. Dougherty J.E., Porteous R.K., Kilgore M. D., Graves D.B. // *J. Appl. Phys.*, 1992, vol. 72, p. 3934.
17. Tsytovich V.N., Khodatayev Ya.K., Bingham R. // *Comments Plasma Phys. and Control. Fusion*, 1996, vol. 17, p. 249.
18. Bystrenko T., Zagorodny A. // *Ukr. J. Phys.*, 2002, vol. 47, No.4, p. 341.
19. Goree J. // *Phys. Rev. Lett*, 1992, vol. 69, p. 277.
20. Lampe M., Joyce G., Ganguli G., Gavrishchaka V. // *Phys. Plasmas*, 2000, vol. 7, p. 3851.
21. Lampe M., Gavrishchaka V., Ganguli G., Joyce G. // *Phys. Rev. Lett.*, 2001, vol. 86, p. 5378.
22. Lampe M. et al. – In: *Proceedings of the Second Capri Workshop on Dusty Plasmas*, Ed. by U. de Angelis and C. Nappi, 2001, No. 13.
23. Zobnin A.V., Nefedov A. P., Sinel'shchikov V.A., Fortov V.E. // *JETP*, 2000, vol. 91, p. 483.
24. Pal' A.F., Starostin A.N., Filippov A.V. // *Plasma Physics Reports*, 2001, vol. 27, p. 143; *Fizika Plasmy*, 2001, vol. 27, p. 155 (in Russian).
25. Pal' A.F., Serov A.O., Starostin A.N. et al. // *JETP*, 2001, vol. 92, p. 235.
26. Pal' A.F., Sivokhin D.V., Starostin A.N., Filippov A.V., Fortov V.E. // *Plasma Physics Reports*, 2002, vol. 28, p. 28; *Fizika Plazmy*, 2002, vol. 28, p. 32 (in Russian).
27. Bystrenko O., Zagorodny A. // *Phys. Lett. A*, 1999, vol. 255, p. 325; *Condens. Matter Phys.*, 1998, vol. 1, p. 169.
28. Bystrenko O., Zagorodny A. // *Phys. Lett. A*, 1999, vol. 262, p. 72.
29. Bystrenko O., Zagorodny A. // *Phys. Lett. A*, 2000, vol. 274, p. 47.
30. Bystrenko T., Zagorodny A. // *Phys. Lett. A*, 2002, vol. 299, p. 383.
31. Bystrenko O., Zagorodny A. (to be published).
32. Roberts S.M., Shipman J.S. *Two Point Value Problems: Shooting Methods*. New York, Elsevier, 1972.
33. *Monte-Carlo Methods in Statistical Physics*. Ed. K.Binder. Springer, 1979.
34. Schram P.P.J.M., Trigger S.A. // *Contrib. Plasma Phys.*, 1997, vol. 37, p. 251.
35. Löwen H., Madden P.A., Hansen J.P. // *Phys. Rev. Lett.*, 1992, vol. 68, p. 1081.
36. Ewald P. // *Ann. d. Phys.*, 1921, vol. 64, p. 253.
37. Tsytovich V.N., Havnes O. // *Comm. Plasma Phys. Contr. Fusion*, 1993, vol. 14, p. 267.
38. Konopka U., Morfill G.E., Ratke L. // *Phys. Rev. Lett.*, 2000, vol. 84 p. 891.

39. Hockney R.W., Eastwood J.W. Computer Simulations Using Particles. McGraw-Hill, 1981.
40. Chandrasekar S. // Rev. Mod. Phys., 1943, vol. 15, p. 1.
41. Hacken H. Synergetics. Berlin, Springer-Verlag, 1978.

Екранування сильнозаряджених макрочастинок та споріднені явища в колоїдній плазмі

О.Бистренко, Т.Бистренко, А.Загородній

Інститут теоретичної фізики ім. М.М.Боголюбова НАН України
03143 Київ, вул. Метрологічна, 14б

Отримано 3 квітня 2003 р.

Подано стислий виклад важливих останніх результатів по екрануванню сильнозаряджених домішок в колоїдній плазмі. В центрі уваги огляду – нелінійне екранування та його вплив на структуру колоїдної плазми, роль зв'язаних іонів в екрануванні макрочастинок та ефекти сильних зіткнень в плазмовому середовищі. Показано, що ці явища можуть сильно впливати на властивості екранування макрочастинок, призводячи до значних відхилень від традиційної теорії Дебая-Гюкеля, в залежності від фізичних процесів у плазмовому середовищі.

Ключові слова: *сильнозаряджена домішка, заряджена колоїдна суспензія, запорошена плазма, нелінійне екранування, зв'язані іонні стани, сильні зіткнення*

PACS: 52.25.Vy, 52.27.Lw, 52.65.-y

